c-JUN promotes BCR-ABL–induced lymphoid leukemia by inhibiting methylation of the 5′ region of *Cdk6*

Karoline Kollmann,[1,2] Gerwin Heller,[3] Rene Georg Ott,[1] Ruth Scheicher,[1] Eva Zebedin-Brandl,[1] Christine Schneckenleithner,[1,2] Olivia Simma,[1] Wolfgang Warsch,[1] Eva Eckelhart,[1] Andrea Hoelbl,[1] Martin Bilban,[4] Sabine Zöchbauer-Müller,[3] Marcos Malumbres,[5] and Veronika Sexl[1,2]

[1]Institute of Pharmacology, Center of Biomolecular Medicine and Pharmacology, Medical University of Vienna, Vienna, Austria; [2]Institute of Pharmacology and Toxicology, Veterinary University of Vienna, Vienna, Austria; [3]Clinical Division of Oncology, Department of Medicine I, Comprehensive Cancer Center, and [4]Department of Laboratory Medicine, Medical University of Vienna, Vienna, Austria; and [5]Cell Division and Cancer Group, Molecular Oncology Programme, Centro Nacional de Investigaciones Oncológicas, Madrid, Spain

The transcription factor c-JUN and its upstream kinase JNK1 have been implicated in BCR-ABL–induced leukemogenesis. JNK1 has been shown to regulate BCL2 expression, thereby altering leukemogenesis, but the impact of c-JUN remained unclear. In this study, we show that JNK1 and c-JUN promote leukemogenesis via separate pathways, because lack of c-JUN impairs proliferation of *p185*$^{BCR-ABL}$–transformed cells without affecting their viability. The decreased proliferation of *c-Jun*$^{\Delta/\Delta}$ cells is associated with the loss of cyclin-dependent kinase 6 (CDK6) expression. In *c-Jun*$^{\Delta/\Delta}$ cells, CDK6 expression becomes downregulated upon BCR-ABL–induced transformation, which correlates with CpG island methylation within the 5′ region of *Cdk6*. We verified the impact of *Cdk6* deficiency using *Cdk6*$^{-/-}$ mice that developed BCR-ABL–induced B-lymphoid leukemia with significantly increased latency and an attenuated disease phenotype. In addition, we show that reexpression of CDK6 in BCR-ABL–transformed *c-Jun*$^{\Delta/\Delta}$ cells reconstitutes proliferation and tumor formation in *Nu/Nu* mice. In summary, our study reveals a novel function for the activating protein 1 (AP-1) transcription factor c-JUN in leukemogenesis by antagonizing promoter methylation. Moreover, we identify CDK6 as relevant and critical target of AP-1–regulated DNA methylation on BCR-ABL–induced transformation, thereby accelerating leukemogenesis. (*Blood*. 2011;117(15):4065-4075)

Introduction

Activating protein 1 (AP-1) functions as a dimeric transcription factor in important cellular processes such as proliferation, differentiation, and apoptosis.[1-3] This wide range of different roles is made possible by the variable compositions of many homo- and heterodimers that are formed by the JUN, FOS, ATF, and MAF proteins that comprise the AP-1 transcription factors.[4,5]

c-JUN was originally identified as the normal cellular counterpart of the avian sarcoma JUN oncoprotein (v-JUN). Mouse model experiments revealed the essential role of c-JUN for development. *c-Jun*$^{-/-}$ mice die at embryonic day 12.5-13.5, displaying multiple defects in liver, heart, and neural crest.[6,7] c-JUN was shown to transform cells in culture,[6-8] and is commonly expressed at high levels in human malignancies.[9,10] High levels of c-JUN have been described in a large fraction of human melanoma samples,[11] liposarcomas,[12] and lymphomas[13] and are important players in skin and liver tumorigenesis.[14,15] The tumor-promoting roles of c-JUN have been attributed either to growth-accelerating effects via the regulation of CYCLIN expression[16] or to antiapoptotic properties. In hepatocytes, c-JUN antagonizes the function of the tumor-suppressor protein p53 and protects transformed hepatocytes from cell death.[17] In T cells, c-JUN is involved in the expression of the FAS ligand (FASL), triggering apoptosis through the FAS receptor.[18]

In BCR-ABL–driven leukemogenesis, both c-JUN and its upstream regulator JNK1 have been described as tumor promoters.[19-22] For *JNK1*$^{-/-}$–transformed cells, the underlying mechanism has been elucidated: *JNK1*$^{-/-}$ cells express severely reduced levels of the antiapoptotic protein BCL2, which leads to a significantly delayed leukemogenesis in BCR-ABL–transformed cells.[21] However, it remained unclear whether this effect was mediated via c-JUN–dependent phosphorylation.

DNA methylation and modifications of histone proteins such as acetylation or methylation regulate gene expression by affecting the binding of transcription factors to DNA via changes in the structure of chromatin (ie, c-MYC).[23] This may either result in gene activation or gene silencing. Alterations of epigenetic marks, especially of DNA methylation, have been associated with all stages of tumor formation and progression. DNA methylation implicates the covalent addition of a methyl group to the 5′ carbon of cytosine bases within cytosine-guanine (CpG) dinucleotides. Regions in the genome where the CpG dinucleotide occurs at high density are called CpG islands (CGIs), and can be found in approximately 60% of the human gene promoter regions extending into the 5′-coding end of the gene. Whereas 70% to 80% of all non-CGI CpG dinucleotides in the human genome are methylated, CGI CpG dinucleotides usually remain unmethylated. In general, CGI methylation is associated with transcriptional gene silencing.[24-26]

We describe a novel mechanism through which the AP-1 transcription factor modulates tumorigenesis. In B-lymphoid cells, c-JUN counteracts the BCR-ABL–induced DNA methylation within the 5′ region of *Cdk6*, thereby preventing the BCR-ABL–induced

Submitted July 30, 2010; accepted January 9, 2011. Prepublished online as *Blood* First Edition paper, February 7, 2011; DOI 10.1182/blood-2010-07-299644.

The online version of this article contains a data supplement.

The publication costs of this article were defrayed in part by page charge payment. Therefore, and solely to indicate this fact, this article is hereby marked "advertisement" in accordance with 18 USC section 1734.

silencing of the *CDK6* gene. A lack of regulation or down-regulation of CDK6 is associated with a pronounced increase of disease latency, as verified by the use of *Cdk6*$^{-/-}$ mice. Our study reveals primary insights into the role of AP-1 transcription factors for oncogene-induced gene silencing. Moreover, we provide the first conclusive evidence for a nonredundant tumor-promoting role of CDK6 in lymphoid malignancies.

Methods

Mice and infection of neonatal mice with Ab-MuLV

c-Jun$^{fl/fl}$,[27] *CD19-Cre*$^{+/-}$,[28] *Jnk1*$^{-/-}$,[29] *c-Jun*$^{AA/AA}$,[30] *p53*$^{-/-}$,[31] *Cdk6*$^{-/-}$,[32] *Nu/Nu*, and *Rag2*$^{-/-}$ mice[33] have been described previously. Animal experiments were performed in accordance with protocols approved by the animal welfare committee of the Medical University of Vienna.

Newborn mice were injected IP with 50 μL of replication-incompetent ecotropic retrovirus encoding for Ab-MuLV.[34] Sick mice were killed. Peripheral blood, lymphoid tissues, and hematopoietic organs were analyzed for leukemic cells by FACS and by histopathology.

Cell culture, infection of fetal liver cells, and expression vectors

Tissue-culture conditions, virus preparation, infections, transformation assays, and establishment of cell lines were performed as described previously.[13,34,35] The expression vectors used for the experiments were *pMSCV-puro*, *pMSCV-Cdk6-puro*, and *pMSCV-Bcl2-puro.*

Transplantation of tumor cells into *Rag2*$^{-/-}$ and *Nu/Nu* mice

For tail-vein injections, a defined cell number from independently derived *pMSCV-p185*$^{BCR-ABL}$*-IRES-GFP*–transformed cell lines was injected into *Rag2*$^{-/-}$ mice. For subcutaneous injections, 1×10^6 cells were injected into *Nu/Nu* mice. Sick mice were killed and analyzed for spleen weights, white blood cell counts, and the presence of leukemic cells in BM, spleen, liver, and blood by FACS analysis.

[^{3}H]-thymidine incorporation

Cells (5×10^4) were plated in triplicate in 96-well plates and [^{3}H]-thymidine (0.1 μCi/well [MBq/well]) was added. After 12 hours of incubation, analysis was performed with Ultima Gold MV scintillation fluid (Packard Instruments) using a scintillation counter.

Flow cytometric analysis

FACS analysis was performed using a FACSCanto flow cytometer using FACSDiva software (BD Biosciences).

B-cell development staining

We used different antibodies to determine the specific B-lineage maturation stages: B220 (CD45R; RA3-6B2), CD43 (1B11), CD19 (1D3), BP-1 (6C3), IgM (R6-60.2), and IgD^b (IgH-5b; 217-170), all from BD Pharmingen.

Cell-cycle analysis

Cells (5×10^6) were stained with propidium iodide (50 μg/mL) in a hypotonic lysis solution (0.1% sodium citrate, 0.1% Triton X-100, and 100 μg/mL RNAse) and incubated at 37°C for 30 minutes.

Protein analysis and Western blotting

Cells were lysed in a buffer containing protease and phosphatase inhibitors (50mM HEPES, pH 7.5, 0.1% Tween 20, 150mM NaCl, 1mM EDTA, 20mM β-glycerophosphate, 0.1mM sodium vanadate, 1mM sodium fluoride, 10 μg/mL aprotinin, 10 μg/mL leupeptin, and 1mM PMSF). Protein concentrations were determined using a bicinchoninic acid kit (Pierce). Proteins (100 μg) were separated on 12% SDS-PAGE gels and transferred onto Immobilon membranes. Membranes were probed with antibodies directed against CDK6 (C8343) and β-ACTIN (A-4700), both from Sigma-Aldrich; and c-JUN (sc-1694x), p53 (sc-6243), BCL2(sc-7382), CDK4 (sc-260), p21 (sc-471), p27 (sc-1641), p15^{INK4b} (sc-612), and p16^{INK4a} (sc-1207), all from Santa Cruz Biotechnology. Immunoreactive bands were visualized by chemiluminescent detection (ECL detection kit; Amersham).

Treatment with Aza-dC

Cells were seeded in 1μM 5-aza-2′-deoxycytidine (Aza-dC; Sigma-Aldrich). After 12, 24, 36, and 48 hours of incubation, Western blot analysis was performed.

RNA isolation and real-time RT-PCR analysis

RNA was isolated using TRIzol (Invitrogen). First-strand cDNA synthesis and PCR amplification were performed using a RT-PCR kit (GeneAmp RNA PCR kit; Applied Biosystems) according to the manufacturer's instructions. Real-time RT-PCR was performed on a RealPlex cycler using RealMasterMix (Eppendorf) and SYBR Green, as described previously.[36] The following primer pairs were used: *Gapdh*: 5′-AGAAGGTGGTGAAGCAGGCATC-3′ and 5′-CGGCATCGAAGGTGGAAGAGTG-3′ and *Cdk6*: 5′-GCTTCGTGGCTCTGAAGCGCG-3′ and 5′-TGGTTTCTGTGGGTACGCCGG-3′.

Real-time RT-PCR for *Dnmt*

Total RNA (1 μg) was used for cDNA preparation using the Omniscript RT kit (QIAGEN). Real-time RT-PCR of *Dnmt1*, *Dnmt3a*, and *Dnmt3b* was performed using Taqman gene expression assays (Applied Biosystems), as recommended by the manufacturer. *Gapdh* was used as a reference gene for normalization of RT-PCR data.

Nucleic acid isolation, MSP, and bisulfite genomic sequencing

Genomic DNA was isolated from murine *c-Jun*$^{fl/fl}$ and c-*Jun*$^{\Delta/\Delta}$ cell lines by digestion with proteinase K, followed by standard phenol-chloroform extraction and ethanol precipitation. Afterward, 1 μg of genomic DNA was used for chemical modification by sodium bisulfite using the EpiTect kit (QIAGEN). The methylation status of the region 5′ to the coding sequence of *Cdk6* (ENSMUSG00000040274, www.ensembl.org, release 52) was analyzed by methylation-specific PCR (MSP). MSP primers sequences were designed using the MethPrimer program[37] and are as follows: *Cdk6*m-fwd, 5′-TAGTTCGGCGGTCGCGAGTTCG-3′, *Cdk6*m-rev, 5′-CGCACGCGCTTCAAAACCACG-3′, *Cdk6*u-fwd, 5′-TAGTTTGGTGGTTGTGAGTTTG-3′ and *Cdk6*u-rev, 5′-TCACACACACTTCAAAACCACA-3′. PCR was performed under the following conditions: initial denaturation for 12 minutes at 95°C, followed by 38 cycles of denaturation for 30 seconds at 95°C, annealing for 40 seconds at 64°C, and extension for 30 seconds at 72°C, with a final extension for 7 minutes at 72°C. MSP products were separated in 2% agarose gels stained with GelRed (Biotium), and visualized under UV spectrophotometry. DNA extracted from murine cell lines was treated with Sss1 CpG methylase (New England Biolabs) and was used as a positive control for methylated alleles. Water blanks were used as negative controls.

For bisulfite genomic sequencing, PCR primers were designed to anneal at both methylated and unmethylated bisulfite-converted DNA: *Cdk6*-seq-f, GAAGGATAGTTTGAGTYGYGT and *Cdk6*-seq-r, TAACTACCCRAAAACCACCRCA. PCR products were gel excised and cloned using the TOPO cloning kit (Invitrogen). Ten clones of each *c-Jun*$^{fl/fl}$ and *c-Jun*$^{\Delta/\Delta}$ cell were sequenced using M13 reverse primers.

Statistical analysis

Data are reported as mean values ± SEM. Biochemical experiments were performed in triplicate, and a minimum of 3 independent experiments was evaluated. Differences were assessed for statistical significance by an unpaired 2-tailed *t* test or the log-rank test (for Kaplan-Meier plots).

Results

JNK1 and c-JUN are involved in BCR-ABL–induced transformation

The AP-1 upstream kinase JNK1 and the AP-1 transcription factor c-JUN have been implicated in BCR-ABL–driven leukemogenesis.[19,21,22] We confirmed these previous observations by performing colony formation assays in growth factor–free methylcellulose. Fetal liver cells were prepared from *Jnk1*$^{-/-}$ and *c-Jun*$^{fl/fl}$*CD19-Cre*$^{+/-}$ embryos and the appropriate controls, and infected with a retrovirus encoding *p185*$^{BCR\text{-}ABL}$ (*pMSCV-p185*$^{BCR\text{-}ABL}$ *-IRES-GFP*). As expected, a significant reduction of growth factor–independent colony numbers was detected when *Jnk1*$^{-/-}$ or *c-Jun*$^{fl/fl}$*CD19-Cre*$^{+/-}$ hematopoietic cells were used (Figure 1A-B). After transformation, CD19^{+}/CD43^{+} leukemic cell lines were generated from all cultures.

The lack of *Jnk1* has been reported to be associated with an increased disease latency.[21] To study tumor cell–intrinsic characteristics in vivo, we transplanted established cell lines via tail-vein injection into *Rag2*$^{-/-}$ mice. This procedure inflicts a rapidly evolving leukemia, which can be readily monitored in *Rag2*$^{-/-}$ mice because they lack all lymphoid cells except natural killer cells. After injection of *c-Jun*$^{fl/fl}$*CD19-Cre*$^{+/-}$ (*c-Jun*$^{\Delta/\Delta}$) and *c-Jun*$^{fl/fl}$ stable cell lines via the tail vein, the mice developed leukemia with infiltrations of leukemic cells in BM, spleen, liver, and lymph nodes (data not shown). As summarized in Figure 1C, leukemia evolved with a significantly enhanced latency in mice that had received *c-Jun*$^{\Delta/\Delta}$ cells. The signs of disease were attenuated, as evident from the reduced spleen weight of mice suffering from a *c-Jun*–deficient leukemia (Figure 1D).

JNK1 and c-JUN act via different pathways in promoting BCR-ABL–induced leukemia

The lack of *Jnk1* in BCR-ABL–transformed cells was reported to decrease BCL2 expression, which was verified as the major cause for the reduced malignancy of *Jnk1*$^{-/-}$ cells on BCR-ABL transformation. Transgenic expression of *Bcl2* in these cells rescued apoptosis and restored tumors.[21] BCL2 protein expression was also reduced in *c-Jun*$^{\Delta/\Delta}$ cells compared with *c-Jun*$^{fl/fl}$ control cells (Figure 2A). To explore whether the reduction in BCL2 expression accounts for a delayed tumorigenesis in *c-Jun*$^{\Delta/\Delta}$ cells, we expressed BCL2, encoded by a retrovirus, in BCR-ABL–transformed *c-Jun*$^{\Delta/\Delta}$ and *c-Jun*$^{fl/fl}$ cells (Figure 2B bottom panel). Leukemia formation was then investigated by injecting these cells into *Rag2*$^{-/-}$ animals via the tail vein. Surprisingly, disease latency was unaffected whether we injected *c-Jun*$^{\Delta/\Delta}$ cells or *c-Jun*$^{fl/fl}$ cells expressing low or high levels of BCL2 (Figure 2B top panel and supplemental Figure 1A, available on the *Blood* Web site; see the Supplemental Materials link at the top of the online article).

To investigate further whether JNK1 and c-JUN act in a signaling cascade independently of BCL2, we made use of *c-Jun*$^{AA/AA}$ mice harboring point mutations at the critical serine sites subjected to phosphorylation by JNK. Newborn *c-Jun*$^{AA/AA}$ mice and the appropriate controls were infected IP with the replication-deficient retrovirus Ab-MuLV encoding *v-Abl*. As an additional control, we used *c-Jun*$^{fl/fl}$*CD19-Cre*$^{+/-}$ and compared them with *c-Jun*$^{fl/fl}$ mice. Ab-MuLV infects B-lymphoid precursors and induces a slowly evolving pro–B-cell leukemia in mice. Therefore, in contrast to leukemia inflicted by transplanting readily established cell lines by IV injection, disease development is much slower and is induced with delayed kinetics. As depicted in Figure 2C, *c-Jun*$^{fl/fl}$*CD19-Cre*$^{+/-}$ mice developed leukemia with a significantly enhanced latency compared with *c-Jun*$^{fl/fl}$ mice, which is clearly in agreement with the tumor-promoting effect of c-JUN. However, no effect was observed when we compared *c-Jun*$^{AA/AA}$ mice with control animals (Figure 2D). The slight difference in latency between the control mice in these 2 experiments was caused by minor background differences in the animals. In agreement with this, we failed to detect any alteration in the outgrowth of *c-Jun*$^{AA/AA}$ and control *p185*$^{BCR\text{-}ABL}$–transformed cell lines (data not shown). These data indicate that JNK1 and c-JUN promote BCR-ABL–driven tumorigenesis independently using different mechanisms.

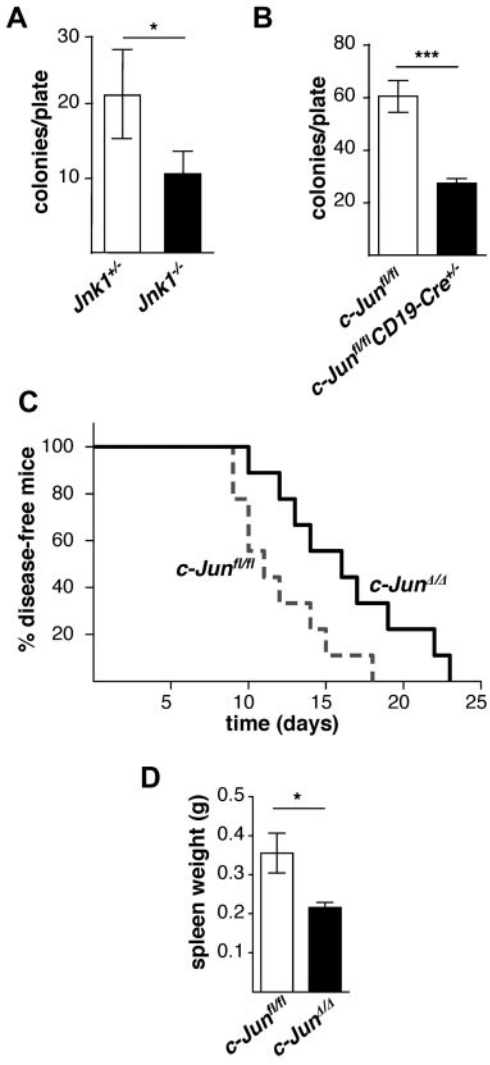

Figure 1. c-JUN is involved in *p185*$^{BCR\text{-}ABL}$-induced transformation and leukemogenesis. Colony formation assays were performed using 1×10^6 (A) *JNK1*$^{+/-}$ and *JNK1*$^{-/-}$ (n = 8; 2-tailed *t* test, 49.2 ± 7.9 vs 28.9 ± 4.1 colonies/10^7 fetal liver cells, *P* = .0401) and (B) *c-Jun*$^{fl/fl}$ and *c-Jun*$^{fl/fl}$*CD19-Cre*$^{+/-}$ (n = 6; 2-tailed *t* test, 60.5 ± 6.1 vs 27.3 ± 1.9 colonies/10^7 fetal liver cells, *P* = .0004) fetal liver cells after infection with a *pMSCV-p185*$^{BCR\text{-}ABL}$*-IRES-GFP* retrovirus in growth factor–free methylcellulose. (C) Transplantation of 1×10^5 *c-Jun*$^{fl/fl}$ and *c-Jun*$^{\Delta/\Delta}$ cells into *Rag2*$^{-/-}$ mice. Two independent cell lines for each cell type were injected in 9 mice (mean survival, 11 vs 16 days in mice injected with *c-Jun*$^{fl/fl}$ and *c-Jun*$^{\Delta/\Delta}$ cells, respectively, *P* = .0307). (D) Spleen weights of diseased recipient *Rag2*$^{-/-}$ mice were analyzed (*c-Jun*$^{fl/fl}$ [n = 9] and *c-Jun*$^{\Delta/\Delta}$ [n = 9], 2-tailed *t* test, *P* = .0169).

c-Jun deficient cells show a proliferative defect

AP-1 members regulate survival, differentiation and proliferation.[15] Because the enforced expression of BCL2 did not accelerate

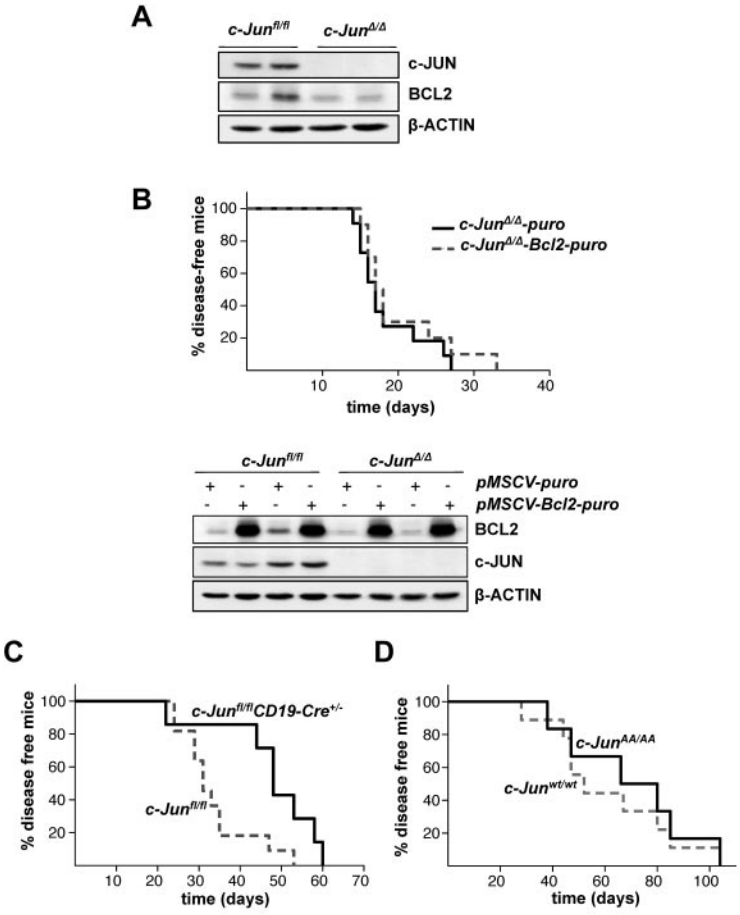

Figure 2. Enforced BCL2 expression does not alter c-JUN–deficient leukemogenesis. (A) Protein levels of c-JUN and BCL2 in *c-Jun*$^{fl/fl}$ and *c-Jun*$^{\Delta/\Delta}$ *p185*$^{BCR\text{-}ABL}$-transformed cells. β-ACTIN served as the loading control. (B) 1×10^5 leukemic *c-Jun*$^{\Delta/\Delta}$ B cells, transduced either with *pMSCV-puro* or *pMSCV-Bcl2-puro*, were injected IV into *Rag2*$^{-/-}$ mice (n = 11 and n = 13, respectively; mean survival, 17 vs 17.5 days in mice injected with *c-Jun*$^{\Delta/\Delta}$*-puro* and *c-Jun*$^{\Delta/\Delta}$*-Bcl2-puro* cells, $P = .3552$) (top panel). Immunoblot analysis shows the enforced expression of BCL2 on a *pMSCV-Bcl2-puro* retrovirus infection in *c-Jun*$^{fl/fl}$ and *c-Jun*$^{\Delta/\Delta}$ cells. β-ACTIN served as the loading control (bottom panel). (C) Injection of *c-Jun*$^{fl/fl}$ (n = 11) and *c-Jun*$^{fl/fl}$*CD19-Cre*$^{+/-}$ (n = 7) newborn mice with a replication-deficient Ab-MuLV–encoding retrovirus resulted in B-lymphoid leukemia/lymphoma (mean survival 31 vs 48 days in *c-Jun*$^{fl/fl}$ and *c-Jun*$^{fl/fl}$*CD19-Cre*$^{+/-}$ mice, respectively, $P = .0173$). (D) Injection of *c-Jun*$^{wt/wt}$ (n = 9) and *c-Jun*$^{AA/AA}$ (n = 6) newborn mice with a replication-deficient Ab-MuLV–encoding retrovirus resulted in B-lymphoid leukemia/lymphoma (mean survival 52 vs 73 days in *c-Jun*$^{wt/wt}$ and *c-Jun*$^{AA/AA}$ mice, respectively, $P = .6168$).

leukemogenesis in *c-Jun*$^{\Delta/\Delta}$ cells, we next investigated cell growth of BCR-ABL–transformed *c-Jun*$^{\Delta/\Delta}$ cells. Six individually derived, stable cell lines lacking *c-Jun* and corresponding control cell lines were generated. [^{3}H]-thymidine incorporation assays and growth curves showed a significant difference in the proliferation of *c-Jun*$^{\Delta/\Delta}$ and *c-Jun*$^{fl/fl}$ cells. *c-Jun*$^{\Delta/\Delta}$ cells expanded significantly more slowly (Figure 3A-B). This was also evident from the DNA content of asynchronously proliferating cells: *c-Jun*$^{\Delta/\Delta}$ cells showed a significantly increased proportion of cells in the G_1 phase and a decreased proportion in the S phase (Figure 3C). To monitor tumor growth in vivo, we made use of *Nu/Nu* mice. Tumor cells were injected subcutaneously to allow monitoring of tumor growth. These in vivo experiments recapitulated the in vitro observations. *c-Jun*$^{\Delta/\Delta}$ tumors evolved significantly more slowly in *Nu/Nu* mice. The experiment was terminated after 10 days, when the first tumor reached 1 cm in diameter. At that time, the weight of the *c-Jun*$^{\Delta/\Delta}$ tumors compared with the *c-Jun*$^{fl/fl}$ tumors was significantly lower (Figure 3D).

In hepatocytes, c-JUN accelerates tumor formation by antagonizing the proapoptotic activity of p53.[17] A role for p53 has been established for BCR-ABL–induced disease previously. BCR-ABL–induced transformation and leukemia occur more rapidly on a *p53*$^{-/-}$ background because the cells do not have to overcome p53-induced apoptosis and crisis induced by oncogenic stress.[38] To determine the possible involvement of c-JUN in this mechanism and to find out whether c-JUN is required to counteract the proapoptotic effects of p53 during transformation, we crossed *c-Jun*$^{fl/fl}$ and *c-Jun*$^{fl/fl}$*CD19-Cre*$^{+/-}$ mice with *p53*$^{-/-}$ mice and then assessed leukemia formation by challenging newborn *c-Jun*$^{fl/fl}$*p53*$^{-/-}$ and *c-Jun*$^{fl/fl}$*CD19-Cre*$^{+/-}$ *p53*$^{-/-}$ mice with Ab-MuLV. As depicted in Figure 2E, *p53* deficiency did not change the disease latency that was observed upon transformation of *c-Jun*$^{fl/fl}$ and *c-Jun*$^{fl/fl}$*CD19-Cre*$^{+/-}$ mice. This experiment led us to conclude that c-JUN is not required to antagonize p53, as is observed in hepatocytes, but rather suggests an involvement of c-JUN in growth control in *p185*$^{BCR\text{-}ABL}$–positive tumor cells.

Transformed c-Jun$^{\Delta/\Delta}$ cells down-regulate the expression of the cell-cycle kinase CDK6

To determine which cell-cycle components are altered in *c-Jun*$^{\Delta/\Delta}$ cell lines, we compared genome-wide gene expression patterns of *c-Jun*$^{fl/fl}$ and *c-Jun*$^{\Delta/\Delta}$ cells using microarray analysis. Microarray results are summarized in a scatter plot in supplemental Figure 2A and in supplemental Tables 1-2. Expression of 31 transcripts was found to be down-regulated at least 2-fold in *c-Jun*$^{\Delta/\Delta}$ cells. These transcripts included the cell-cycle kinase *Cdk6* and the cell-cycle inhibitor and tumor suppressor *p16*^{INK4a}. Microarray data for these genes were confirmed by Western blot analysis (Figure 4A). Loss of CDK6 was restricted to stable *c-Jun*$^{\Delta/\Delta}$ cell lines and was not observed in *p185*$^{BCR\text{-}ABL}$–transformed c-*Jun*$^{AA/AA}$ cells, supporting the independence of JNK phosphorylation (Figure 4B). The protein expression of CDK6 steadily declined after 2, 4, 6, and 8 weeks of the initial transformation event by retroviral infection with *p185*$^{BCR\text{-}ABL}$ in *c-Jun*$^{\Delta/\Delta}$ cells (Figure 4C). This constant protein reduction was correlated with a decrease in the proliferative capacity of the cells (Figure 4D). After 2 weeks, the cell cultures already consisted of more than 95% GFP$^+$ and therefore BCR-ABL$^+$ cells; therefore, a decreasing contamination with nontransformed cells can be ruled out. Quantitative PCR experiments revealed that the reduction of the CDK6 protein

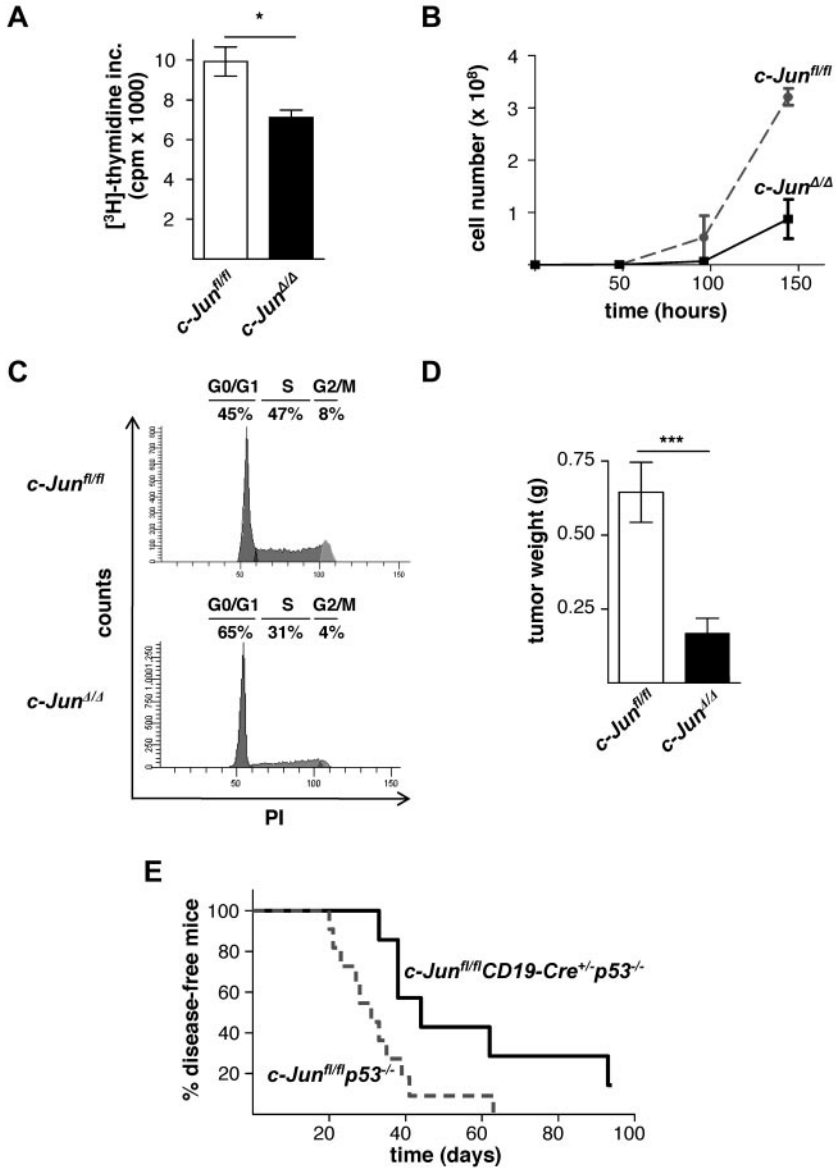

Figure 3. *c-Jun*$^{\Delta/\Delta}$ *p185*$^{\text{BCR-ABL}}$–transformed cell lines demonstrate a proliferative defect. (A) [^{3}H]-thymidine incorporation of fetal liver–derived *c-Jun*$^{\text{fl/fl}}$ (n = 3) and *c-Jun*$^{\Delta/\Delta}$ (n = 4; 2-tailed *t* test, *P* = .0142) *p185*$^{\text{BCR-ABL}}$-transformed cell lines. (B) 1×10^5 *p185*$^{\text{BCR-ABL}}$-transformed *c-Jun*$^{\text{fl/fl}}$ (n = 3) and *c-Jun*$^{\Delta/\Delta}$ cells (n = 3) were plated and total cell numbers were determined after 48, 96, and 144 hours. (C) Cell-cycle profiles of *c-Jun*$^{\text{fl/fl}}$ (n = 5) and *c-Jun*$^{\Delta/\Delta}$ (n = 4) cells (2-tailed *t* test, G_1 phase, *P* = .0333; S phase, *P* = .0173) gated on living cells. One representative set of data is depicted. (D) Tumor weights of *Nu/Nu* mice that were subcutaneously injected with 1×10^6 *c-Jun*$^{\text{fl/fl}}$ and *c-Jun*$^{\Delta/\Delta}$ leukemic cells. Three independent cell lines for each cell type were injected into 9 mice (2-tailed *t* test, *P* = .0007). (E) Injection of *c-Jun*$^{\text{fl/fl}}$*p53*$^{-/-}$ (n = 11) and *c-Jun*$^{\text{fl/fl}}$*CD19-Cre*$^{+/-}$*p53*$^{-/-}$ (n = 7) newborn mice with a replication-deficient Ab-MuLV–encoding retrovirus resulted in B-lymphoid leukemia/lymphoma (mean survival, 31 vs 44 days in *c-Jun*$^{\text{fl/fl}}$*p53*$^{-/-}$ and *c-Jun*$^{\text{fl/fl}}$*CD19-Cre*$^{+/-}$*p53*$^{-/-}$ mice, *P* = .0213).

was accompanied by a loss of *Cdk6* mRNA (Figure 4E). When we compared *Cdk6* mRNA levels in BCR-ABL–transformed wild-type and *c-Jun*$^{\Delta/\Delta}$ cells side by side, we found that mRNA levels developed in opposite directions. Whereas *Cdk6* mRNA was up-regulated in transformed wild-type cells, a significant decline was observed in cells lacking c-JUN (Figure 4E).

Lack of c-JUN leads to methylation within the 5′ region of *Cdk6* in *p185*$^{\text{BCR-ABL}}$–transformed cells

To determine whether epigenetic changes are responsible for the down-regulation of CDK6 in *p185*$^{\text{BCR-ABL}}$–transformed cells, we developed MSP and bisulfite genomic sequencing assays for DNA methylation analysis of the 5′ region of the *Cdk6* gene. As analyzed by MSP, the time-dependent reduction of *Cdk6* mRNA coincided with DNA methylation within the 5′ region of *Cdk6* (Figure 5A top panel). Whereas *Cdk6* methylation was detected in all stable cell lines lacking c-JUN, the *c-Jun*$^{\text{fl/fl}}$ cells were not methylated for this gene (Figure 5A bottom panel). Results obtained with MSP analysis were confirmed by bisulfite genomic sequencing of the *Cdk6* 5′ region in *c-Jun*$^{\text{fl/fl}}$ and *c-Jun*$^{\Delta/\Delta}$ cells. In total, 20 cell clones of each genotype were sequenced (Figure 5B-C). Further confirmation was obtained when we treated the BCR-ABL–transformed *c-Jun*$^{\Delta/\Delta}$ cells with the demethylating agent Aza-dC for 48 hours. As expected, Aza-dC–induced demethylation of DNA resulted in reexpression of CDK6 by 12 hours after treatment (Figure 5D), and most of the cells had entered the G_0/G_1 phase (supplemental Figure 3A) and began to die 12 hours after Aza-dC addition (Figure 5E). Analyzing the mRNA levels of DNA methyltransferases (*Dnmt1*, *Dnmt3a*, and *Dnmt3b*) in *c-Jun*$^{\Delta/\Delta}$ and *c-Jun*$^{\text{fl/fl}}$ cells using real-time RT-PCR showed a significantly higher amount of *Dnmt3b* mRNA in *c-Jun*$^{\Delta/\Delta}$ cells compared with *c-Jun*$^{\text{fl/fl}}$ cells (Figure 5F).

Loss of CDK6 in BCR-ABL–transformed cells recapitulates the phenotype of *c-Jun* deficiency

We next investigated whether the loss of CDK6 accounts for the reduced proliferation of BCR-ABL–transformed *c-Jun*$^{\Delta/\Delta}$ cells, provoking the increased disease latency. To study the contribution of CDK6 to BCR-ABL–induced tumor formation, we used *Cdk6*$^{-/-}$

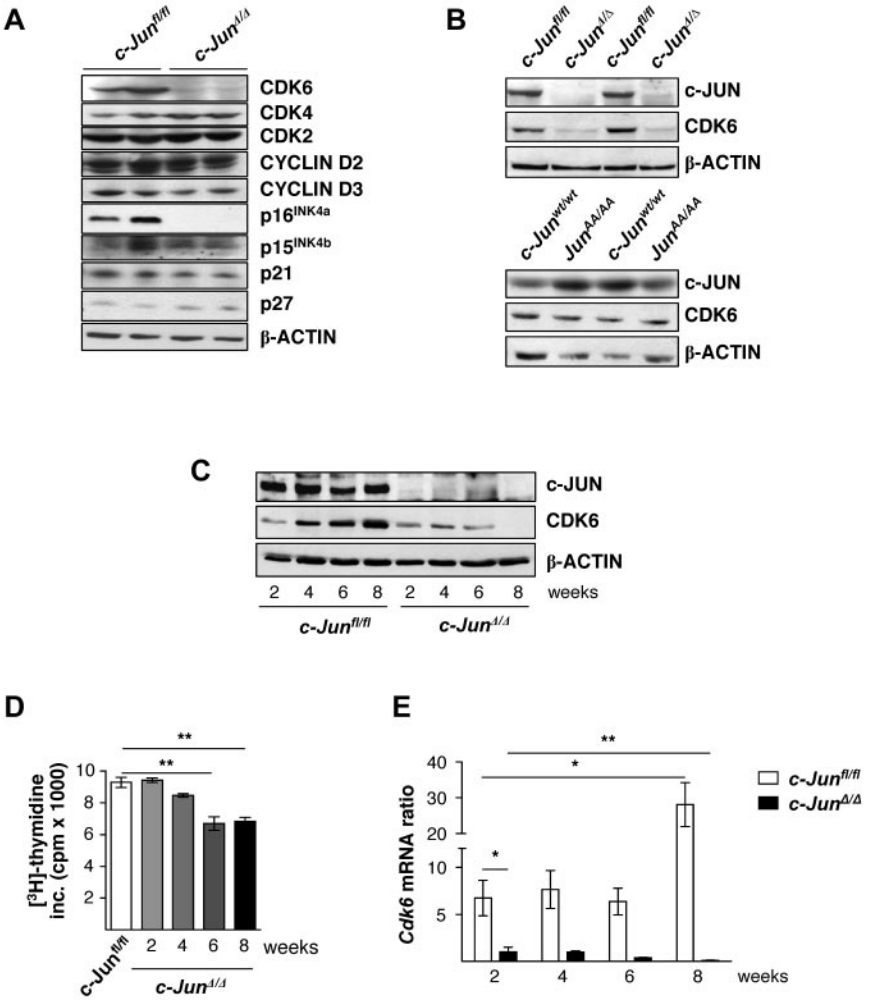

Figure 4. CDK6 protein levels are down-regulated in *c-Jun*$^{\Delta/\Delta}$ *p185*$^{\text{BCR-ABL}}$–transformed cell lines. (A) Immunoblot analysis for CDK6, CDK4, CDK2, CYCLIN D2, CYCLIN D3, p16$^{\text{INK4a}}$, p15$^{\text{INK4b}}$, p21, and p27 protein expression in *c-Jun*$^{\text{fl/fl}}$- and *c-Jun*$^{\Delta/\Delta}$ *p185*$^{\text{BCR-ABL}}$–transformed cells. β-ACTIN served as the loading control. (B) Immunoblot analysis for c-JUN and CDK6 protein expression in *c-Jun*$^{\text{fl/fl}}$ and *c-Jun*$^{\Delta/\Delta}$ (top panel) and *c-Jun*$^{\text{wt/wt}}$ and *c-Jun*$^{\text{AA/AA}}$ (bottom panel) *p185*$^{\text{BCR-ABL}}$–transformed cells. β-ACTIN served as the loading control. (C) c-JUN and CDK6 protein levels of *c-Jun*$^{\Delta/\Delta}$ and *c-Jun*$^{\text{fl/fl}}$ cell lines after 2, 4, 6, and 8 weeks of transformation. β-ACTIN served as the loading control. One representative set of data is depicted. (D) [^{3}H]-thymidine incorporation of the same cell lines was measured (n = 3; 2-tailed *t* test: *c-Jun*$^{\text{fl/fl}}$ vs *c-Jun*$^{\Delta/\Delta}$ 6 weeks, $P = .002$; *c-Jun*$^{\text{fl/fl}}$ vs *c-Jun*$^{\Delta/\Delta}$ 8 weeks, $P = .0016$). (E) *Cdk6* mRNA levels of *c-Jun*$^{\Delta/\Delta}$ and *c-Jun*$^{\text{fl/fl}}$ cells 2, 4, 6, and 8 weeks after *p185*$^{\text{BCR-ABL}}$ transformation were analyzed by quantitative PCR (n = 3; 2-tailed *t* test: *c-Jun*$^{\text{fl/fl}}$ 2 weeks vs *c-Jun*$^{\Delta/\Delta}$ 2 weeks, $P = .0385$; *c-Jun*$^{\text{fl/fl}}$ 2 weeks vs *c-Jun*$^{\text{fl/fl}}$ 8 weeks, $P = .0293$; *c-Jun*$^{\Delta/\Delta}$ 2 weeks vs *c-Jun*$^{\Delta/\Delta}$ 8 weeks, $P = .0024$). The fold change compared with *c-Jun*$^{\Delta/\Delta}$ 2-week *Cdk6* mRNA level is shown. Results were normalized by comparison with their *Gapdh* mRNA expression.

mice. Because no information on a potential role of CDK6 in B-lymphoid development was available, we first monitored the emergence of individually defined B-cell stages. Figure 6A shows typical examples of FACS blots; a summary and a statistical analysis of 4 mice of each genotype is given in Figure 6B. Briefly, *Cdk6*$^{-/-}$ mice had significantly elevated levels of pre–pro-B cells. The total cell number of peripheral mature B cells was unaltered, indicating that this partial block was compensated for in vivo. Mature *Cdk6*$^{-/-}$ B lymphocytes responded equally well to mitogenic stimuli compared with control cells (supplemental Figure 3A). We next transformed fetal liver–derived *Cdk6*$^{-/-}$ cells and wild-type controls with a *pMSCV-p185*$^{\text{BCR-ABL}}$*-IRES-GFP* retrovirus. GFP$^+$CD43$^+$CD19$^+$B220$^+$ colonies and cell lines were obtained with equal frequencies (supplemental Figure 3B). However, a significant difference became obvious in a [^{3}H]-thymidine incorporation assay; a decreased proliferation was also documented by growth curves (Figure 6B-C). These data point toward an essential, nonredundant role for CDK6 in transformed B cells, which is in contrast to the observation in nontransformed, mature B cells, in which the lack of CDK6 did not impair proliferation (supplemental Figure 4A).

To assess tumor formation in vivo, we injected a replication-incompetent retrovirus encoding Ab-MuLV in newborn mice, thereby inducing a slowly emerging lymphoid leukemia. The outcome of the experiment is summarized in Figure 6D. Strikingly, *Cdk6*$^{-/-}$ animals developed disease significantly later and survived the oncogenic challenge up to 5 months, whereas all *Cdk6*$^{+/+}$ and *Cdk6*$^{+/-}$ mice succumbed to leukemia within ~2 months. A slightly decreased infiltration of the spleen with leukemic cells was found in *Cdk6*$^{-/-}$ mice, but this difference did not meet the criteria for being statistically significant (Figure 6E). This experiment highlighted a nonredundant role of CDK6 as a tumor promoter for *p185*$^{\text{BCR-ABL}}$–induced B-cell leukemia. In summary, these data revealed a nonredundant tumor-promoting role for CDK6 in *p185*$^{\text{BCR-ABL}}$–driven leukemogenesis.

Reexpression of CDK6 reconstitutes proliferation in *c-Jun*$^{\Delta/\Delta}$ cells

To define whether the loss of CDK6 accounts for the decreased proliferation and tumor formation of BCR-ABL–transformed *c-Jun*$^{\Delta/\Delta}$ cells, we reexpressed CDK6 with a *pMSCV-Cdk6-puro* retrovirus in *c-Jun*$^{\Delta/\Delta}$ cells (Figure 7A). As depicted in Figure 7B, *c-Jun*$^{\Delta/\Delta}$ cells proliferated significantly faster after CDK6 expression compared with control cells that had been infected with the empty vector. In addition, the proportion of these cells in the G_1 and S phases showed no significant difference compared with *c-Jun*$^{\text{fl/fl}}$ cells (Figure 7C). Tumor formation in *Nu/Nu* mice was assessed with *c-Jun*$^{\Delta/\Delta}$*-Cdk6-puro* cells compared with *c-Jun*$^{\Delta/\Delta}$ cells and in this in vivo experiment, an increased tumor size of *c-Jun*$^{\Delta/\Delta}$*-Cdk6-puro* cells was detected (Figure 7D). We concluded that reexpression of CDK6 in *c-Jun*$^{\Delta/\Delta}$ cells restores proliferation to

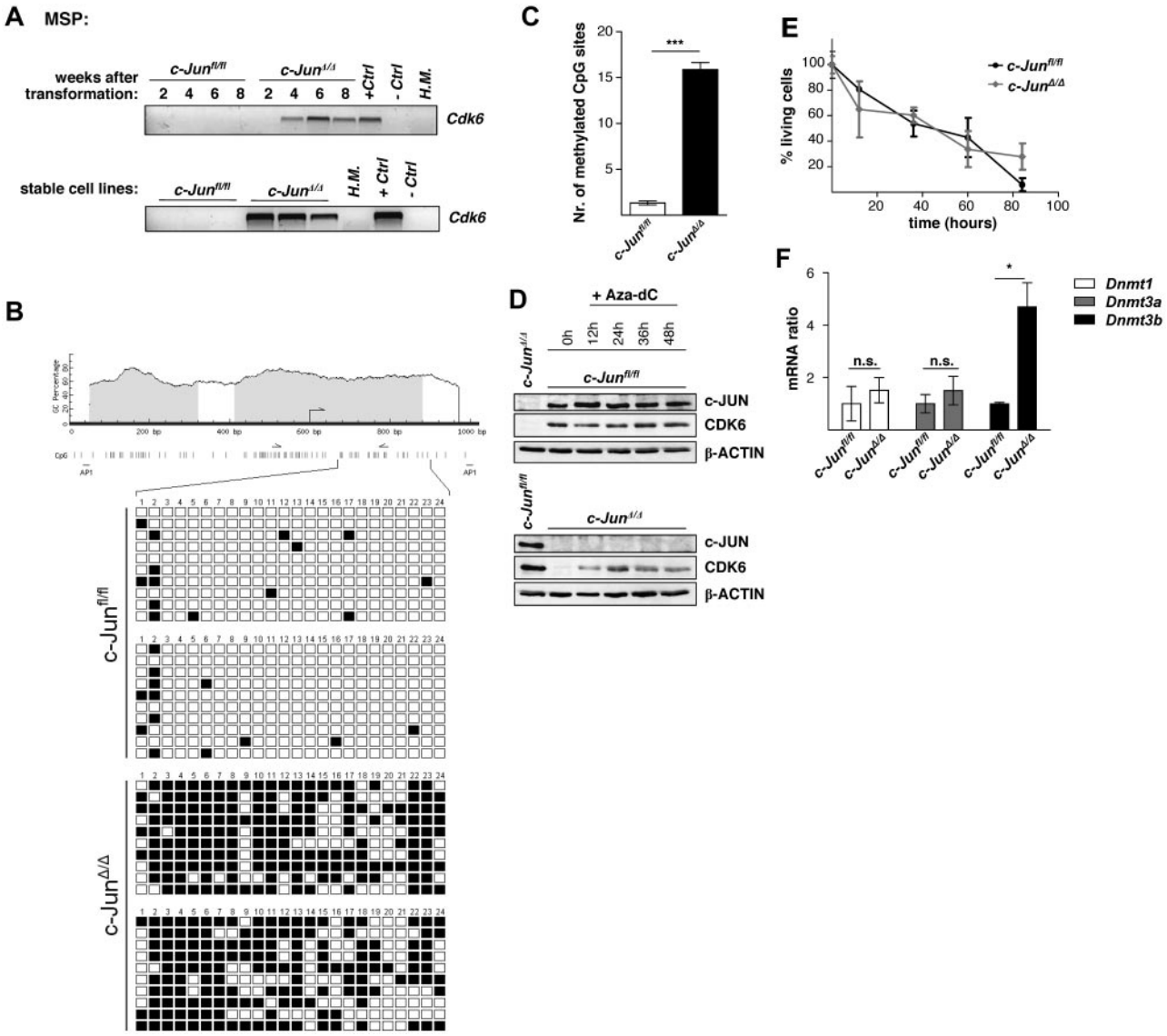

Figure 5. The 5′ region of *Cdk6* is methylated in *c-Jun*$^{\Delta/\Delta}$ cells. (A) Hypermethylation in *c-Jun*$^{fl/fl}$ and *c-Jun*$^{\Delta/\Delta}$ cells after 2, 4, 6, and 8 weeks of *p185*$^{BCR\text{-}ABL}$ transformation (top panel) and in stable *c-Jun*$^{fl/fl}$ and *c-Jun*$^{\Delta/\Delta}$ cell lines (bottom panel), was detected by MSP analysis. A visible PCR product indicates the presence of methylated alleles. *H.M.* indicates BM of a healthy mouse; +Ctrl, control for methylated samples; −Ctrl, control for unmethylated samples. (B) Location of CpG islands within the 5′ region of *Cdk6* (gray boxes). CpG sites are shown as horizontal bars, MSP primer-binding sites are shown as arrows, and AP1-binding sites are shown as vertical bars (black). Twenty-four CpG sites were analyzed by bisulfite genomic sequencing in 2 *c-Jun*$^{fl/fl}$ and in 2 *c-Jun*$^{\Delta/\Delta}$ cell lines. In total, 20 clones of each genotype were sequenced. Small black boxes indicate methylated CpG sites and white boxes indicate unmethylated CpG sites. (C) A statistically significant difference between *Cdk6* methylation in *c-Jun*$^{fl/fl}$ and *c-Jun*$^{\Delta/\Delta}$ cells was observed (n = 20; 2-tailed *t* test, $P < .0001$). (D) Immunoblot for c-JUN and CDK6 of *c-Jun*$^{\Delta/\Delta}$ and *c-Jun*$^{fl/fl}$ cells after 12, 24, 36, and 48 hours of Aza-dC treatment. β-ACTIN served as the loading control. One representative set of data is depicted. (E) Percentage of living cells 12, 36, 60, and 84 hours after Aza-dC treatment of *c-Jun*$^{\Delta/\Delta}$ and *c-Jun*$^{fl/fl}$ leukemic cells. Viability was analyzed by propidium iodide staining. (F) *Dnmt1*, *Dnmt3a*, and *Dnmt3b* mRNA levels of *c-Jun*$^{fl/fl}$ and *c-Jun*$^{\Delta/\Delta}$ cells were analyzed by RT-PCR (n = 3; 2-tailed *t* test, *Dnmt3b*, $P = .016$). The fold change compared with *c-Jun*$^{fl/fl}$ mRNA levels is shown. Results were normalized by comparison with their *Gapdh* mRNA expression.

levels observed in wild-type control cells and accelerates tumor formation in vivo.

Discussion

We have shown that the AP-1 transcription factor c-JUN promotes BCR-ABL–induced leukemogenesis by maintaining the expression of the cell-cycle kinase CDK6. c-JUN is required to protect the CpG island in the 5′ region of *Cdk6* from being methylated. We defined a novel mechanism for how AP-1 transcription factors that are commonly up-regulated in transformed cells contribute to tumorigenesis. Furthermore, we defined for the first time a tumor-promoting role for CDK6 in B-lymphoid leukemogenesis.

Although c-JUN has unequivocally been implicated in the regulation of apoptosis during tumorigenesis,[17] these effects have been excluded for BCR-ABL–induced B-lymphoid leukemogenesis. Neither the enforced expression of BCL2 nor the lack of *p53* counteracted or influenced the effects on disease latency that occurred in the absence of c-JUN during leukemia progression. This is in contrast to the situation in *Jnk1*$^{-/-}$ cells, in which the enforced expression of BCL2 reconstituted leukemogenesis.[21] This also led us to conclude that JNK1 exerts its effects independently of c-JUN, which was further confirmed by investigating *c-Jun*$^{AA/AA}$ mice. How JNK1 regulates BCL2 expression and promotes survival independently of c-JUN remains to be determined.

We cannot rule out that c-JUN exerts a survival function during the initial transformation event. Similar to *Jnk1*$^{-/-}$ cells, *c-Jun*$^{\Delta/\Delta}$

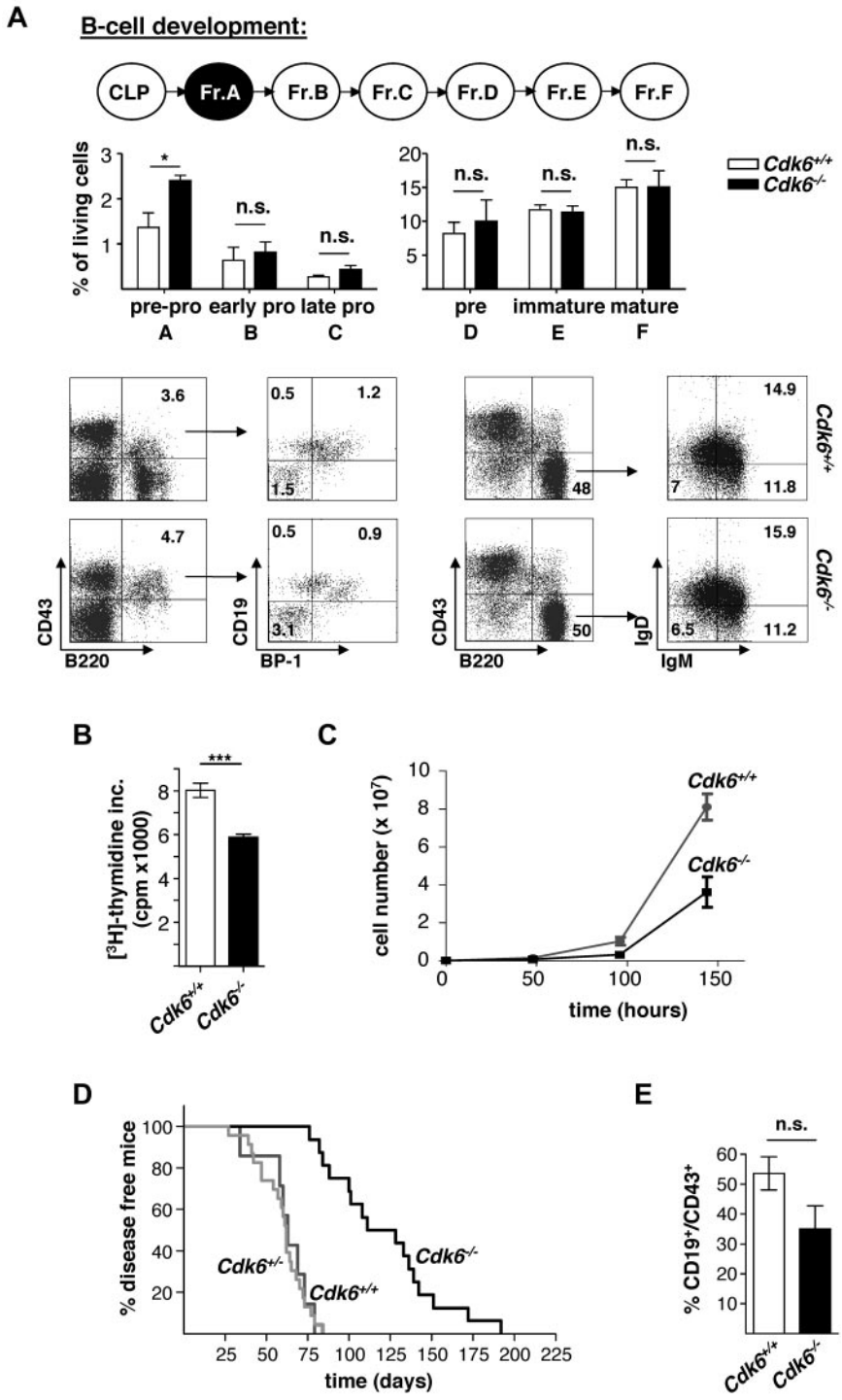

Figure 6. CDK6 advances *p185*$^{BCR\text{-}ABL}$–induced leukemia. (A) Top panel shows the percentages of B cells of fraction A-C in the BM (left panel) and fraction D-F in the spleens (right panel) of *Cdk6*$^{-/-}$ mice compared with *Cdk6*$^{+/+}$ mice as analyzed by FACS (n = 3; fraction A: 2-tailed *t* test, $P = .0379$). In the bottom panel, dot blots indicate the percentages of gated CD43$^+$/B220$^+$ (first panel) and CD43$^+$/B220$^+$/CD19$^-$/BP-1$^-$ for fraction A, CD43$^+$/B220$^+$/CD19$^+$/BP-1$^-$ for fraction B, and CD43$^+$/B220$^+$/CD19$^+$/BP-1$^+$ for fraction C (second panel) in the BM and gated CD43$^-$/B220$^+$ (third panel) and CD43$^-$/B220$^+$/IgD$^-$/IgM$^-$ for fraction D, CD43$^-$/B220$^+$/IgD$^+$/IgM$^-$ for fraction E, and CD43$^-$/B220$^+$/IgD$^-$/IgM$^-$ for fraction F (fourth panel) in the spleens of *Cdk6*$^{-/-}$ and *Cdk6*$^{+/+}$ mice. (B) [^{3}H]-thymidine incorporation into fetal liver–derived *Cdk6*$^{+/+}$ and *Cdk6*$^{-/-}$ *p185*$^{BCR\text{-}ABL}$–transformed cell lines was measured (n = 6; 2-tailed *t* test, $P < .0001$). (C) Cells (1×10^5) of *p185*$^{BCR\text{-}ABL}$–transformed *Cdk6*$^{+/+}$ (n = 3) and *Cdk6*$^{-/-}$ (n = 3) mice were plated and total cell numbers were determined after 48, 96, and 144 hours. (D) Injection of *Cdk6*$^{+/+}$ (n = 7), *Cdk6*$^{+/-}$ (n = 23), and *Cdk6*$^{-/-}$ (n = 16) newborn mice with a replication-deficient Ab-MuLV–encoding retrovirus resulted in B-lymphoid leukemia/lymphoma (mean survival 63 vs 62 vs 120 days in *Cdk6*$^{+/+}$, *Cdk6*$^{+/-}$, and *Cdk6*$^{-/-}$ mice, respectively; $P < .0001$ for *Cdk6*$^{+/+}$ vs *Cdk6*$^{-/-}$). (E) The infiltration rates of CD19$^+$/CD43$^+$ cells in the spleens of diseased mice were analyzed by FACS (n = 6; 2-tailed *t* test, $P = .103$).

cells gave rise to significantly reduced colony numbers when plated in growth factor–free methylcellulose. This is in contrast to our observations in *Cdk6*$^{-/-}$ cells, which display unimpaired colony formation. Obviously, transformation induces rewiring of signaling pathways and changes the signaling network required for survival and proliferation. Therefore, factors that are required within the initial transformation process may become irrelevant for tumor-cell maintenance. This has been recently demonstrated for the transcription factor STAT3.[39]

Interestingly, nontransformed B-lymphoid cells lacking c-JUN express regular levels of CDK6. Only upon transformation with the BCR-ABL oncogene does the 5′ region of *Cdk6* become methylated, if not protected and prevented, by c-JUN. Hundreds of possibly epigenetically silenced genes exist in individual tumors. Whereas a selection for stochastic events certainly exists and selects for dominant tumor clones, it is unlikely that all of these events arise in a random fashion. Rather, the current model suggests that the existence of multiple epigenetically silenced genes reflects a general program of epigenetic control abnormalities. These early epigenetic silencing events could represent primary alterations induced by the initial transformation event. Our data support this model, because the BCR-ABL–induced transformation consistently provoked the

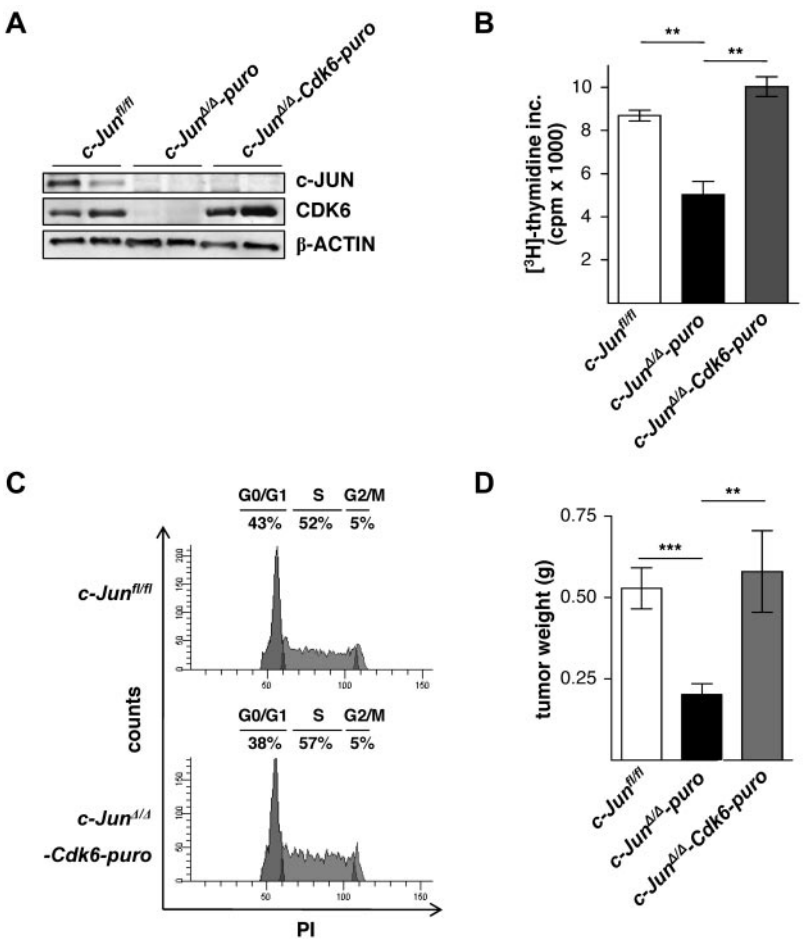

Figure 7. Reexpression of CDK6 in *c-Jun*$^{\Delta/\Delta}$ cells rescues the proliferative defect. (A) Immunoblot analysis of the enforced expression of CDK6 with a *pMSCV-Cdk6-puro* retrovirus in *c-Jun*$^{\Delta/\Delta}$ cells. β-ACTIN served as the loading control. (B) [^{3}H]-thymidine incorporation in *c-Jun*$^{fl/fl}$, *c-Jun*$^{\Delta/\Delta}$*-puro*, and *c-Jun*$^{\Delta/\Delta}$*-Cdk6-puro* cell lines (n = 3; 2-tailed *t* test, *c-Jun*$^{fl/fl}$ vs *c-Jun*$^{\Delta/\Delta}$*-puro*, $P = .0053$; *c-Jun*$^{\Delta/\Delta}$*-puro* vs *c-Jun*$^{\Delta/\Delta}$*-Cdk6-puro*, $P = .0029$). (C) Cell-cycle profiles of *c-Jun*$^{fl/fl}$ (n = 5) and *c-Jun*$^{\Delta/\Delta}$*-Cdk6-puro* (n = 4) cells gated on living cells. One representative set of data is depicted. (D) 1×10^6 *c-Jun*$^{fl/fl}$, *c-Jun*$^{\Delta/\Delta}$*-puro*, and *c-Jun*$^{\Delta/\Delta}$*-Cdk6-puro p185*$^{BCR\text{-}ABL}$–transformed cells were injected subcutaneously into *Nu/Nu* mice. Two independent cell lines for each cell type were injected into mice (2-tailed *t* test, *c-Jun*$^{fl/fl}$ [n = 17] vs *c-Jun*$^{\Delta/\Delta}$*-puro* [n = 17], $P < .0001$; *c-Jun*$^{\Delta/\Delta}$*-puro* [n = 17] vs *c-Jun*$^{\Delta/\Delta}$*-Cdk6-puro* [n = 11], $P = .0017$).

silencing of the C*dk6* gene by DNA methylation. Alternatively, one might suggest that c-JUN is exclusively required for CDK6 expression. In the absence of c-JUN, *Cdk6* transcription comes to a stop, which then induces DNA methylation. The fact that we found increased mRNA levels of the DNA methyltransferases *Dnmt1*, *Dnmt3a*, and *Dnmt3b* in BCR-ABL–transformed *c-Jun*$^{\Delta/\Delta}$ cells suggests a general mechanism not specific for *Cdk6*. It remains to be determined which of the genes found to be down-regulated in the absence of c-JUN in transformed cells have also undergone promoter methylation. Interestingly, the de novo methyltransferase *Dnmt3b* was significantly high in the absence of c-JUN. The enzymes DNMT3a and DNMT3b account for the somatic methylation pattern during embryogenesis and favor semi- and unmethylated DNA substrates.[40,41] In contrast, DNMT1 specifies copying existing methylation patterns.[40,42]

What singles out CDK6 silencing is the fact that CDK6 contributes significantly to the tumor-promoting role of c-JUN. The reduced growth of BCR-ABL–transformed *c-Jun*$^{\Delta/\Delta}$ cells can be largely overridden by the enforced expression of CDK6, which reconstitutes the proliferative ability of the cells and thereby enhances tumor formation in *Nu/Nu* mice. It is also noteworthy that the expression of CDK6 is subject to regulation not only by c-JUN, but also by the related protein JUNB. We have recently found that JUNB suppresses the transcription of *Cdk6* in BCR-ABL–transformed cells.[35] As a consequence, the loss or down-regulation of JUNB—as observed in human myeloid and B-lymphoid malignancies—provokes increased CDK6 expression. In summary, a shift of AP-1 composition occurs in B-lymphoid malignancies: c-JUN becomes up-regulated whereas JUNB remains constant or gets down-regulated.[13] Based on these alterations of AP-1 expression pattern, one might therefore expect an overall increased expression of CDK6 in B-lymphoid malignancies. Indeed, enhanced CDK6 protein expression has been documented in lymphoma and leukemia in humans.[43-46] In particular, several reports have documented chromosomal translocations in patients suffering from B-lymphoid malignancies involving CDK6. In these patients, the aberrant and increased expression of CDK6 had been proposed to represent a cause and/or driving force for the B-cell disease.[47-49] In addition, a recent study describes a down-regulation of the microRNA hsa-miR-124a during acute lymphoblastic leukemia, resulting in an up-regulation of CDK6.[50] Nevertheless, it remained unclear until now whether the enforced expression of CDK6 represents a bystander alteration or is indeed a driving force in B-lymphoid leukemogenesis. We provide the first evidence for the tumor-promoting role by showing that the absence of CDK6 drastically prolonged tumorigenesis in vivo. CDK6 advanced the growth of transformed B-lymphoid cells. *p185*$^{BCR\text{-}ABL}$–induced leukemia was significantly delayed in *Cdk6*$^{-/-}$ mice, and the lifespan of the affected animals nearly doubled. Therefore, in B-lymphoid malignancies, CDK6 exerts a unique and nonredundant tumor-promoting role. CDK6 comes into this privileged position only upon BCR-ABL–induced transformation, after which it takes over the dominant role during the G_1 phase of the cell cycle. It is tempting to speculate that this alteration might be the direct consequence of the changed AP-1 expression profiles and may result from the combination of low or missing JUNB combined with elevated c-JUN expression.

In summary, we provide first insights into a role for the AP-1 transcription factors as modulators of epigenetic reprogramming

occurring in transformed cells. Our data reveal a linear axis for c-JUN and CDK6 in the regulation of proliferation in transformed B-lymphoid cells. In this scenario, CDK6 occupies a privileged and unique position and exerts a nonredundant, tumor-promoting role.

Acknowledgments

We thank Udo Losert and the staff of the Biomedical Research Institute, Medical University of Vienna, as well as Gabriele Schöppl and the mouse facility of the Institute of Pharmacology, Medical University of Vienna, for taking excellent care of the mice. We are grateful to Gerda Egger, Latifa Bakiri, Robert Eferl, Denise Barlow, and Michael Freissmuth for valuable discussions. We thank Erwin F. Wagner for providing essential reagents and mice.

This work was supported by the Vienna Science and Technology Fund (grants LS07-037 and LS07-019) and by the Austrian Science Foundation (grants SFB F28 and P19723 to V.S.).

Authorship

Contribution: K.K., G.H., R.G.O., R.S., E.Z.-B., C.S., O.S., W.W., E.E., A.H., M.B., S.Z.-M., M.M., and V.S. designed and performed research and analyzed data; M.M. provided vital new reagents and analytic tools; and K.K. and V.S. wrote the paper.

Conflict-of-interest disclosure: The authors declare no competing financial interests.

Correspondence: Veronika Sexl, Institute of Pharmacology, and Toxicology, Veterinary University of Vienna, Veterinaerplatz 1, A-1210 Vienna, Austria; e-mail: veronika.sexl@vetmeduni.ac.at.

References

1. Shaulian E, Karin M. AP-1 as a regulator of cell life and death. *Nat Cell Biol.* 2002;4(5):E131-E136.
2. Hess J, Angel P, Schorpp-Kistner M. AP-1 subunits: quarrel and harmony among siblings. *J Cell Sci.* 2004;117(pt 25):5965-5973.
3. Wagner EF, Eferl R. Fos/AP-1 proteins in bone and the immune system. *Immunol Rev.* 2005;208:126-140.
4. Hai T, Curran T. Cross-family dimerization of transcription factors Fos/Jun and ATF/CREB alters DNA binding specificity. *Proc Natl Acad Sci U S A.* 1991;88(9):3720-3724.
5. Chinenov Y, Kerppola TK. Close encounters of many kinds: Fos-Jun interactions that mediate transcription regulatory specificity. *Oncogene.* 2001;20(19):2438-2452.
6. Hilberg F, Aguzzi A, Howells N, Wagner EF. c-jun is essential for normal mouse development and hepatogenesis. *Nature.* 1993;365(6442):179-181.
7. Eferl R, Sibilia M, Hilberg F, et al. Functions of c-Jun in liver and heart development. *J Cell Biol.* 1999;145(5):1049-1061.
8. Jochum W, Passegue E, Wagner EF. AP-1 in mouse development and tumorigenesis. *Oncogene.* 2001;20(19):2401-2412.
9. Zhang W, Hart J, McLeod HL, Wang HL. Differential expression of the AP-1 transcription factor family members in human colorectal epithelial and neuroendocrine neoplasms. *Am J Clin Pathol.* 2005;124(1):11-19.
10. Vleugel MM, Greijer AE, Bos R, van der Wall E, van Diest PJ. c-Jun activation is associated with proliferation and angiogenesis in invasive breast cancer. *Hum Pathol.* 2006;37(6):668-674.
11. Lopez-Bergami P, Huang C, Goydos JS, et al. Rewired ERK-JNK signaling pathways in melanoma. *Cancer Cell.* 2007;11(5):447-460.
12. Mariani O, Brennetot C, Coindre JM, et al. JUN oncogene amplification and overexpression block adipocytic differentiation in highly aggressive sarcomas. *Cancer Cell.* 2007;11(4):361-374.
13. Szremska AP, Kenner L, Weisz E, et al. JunB inhibits proliferation and transformation in B-lymphoid cells. *Blood.* 2003;102(12):4159-4165.
14. Young MR, Li JJ, Rincon M, et al. Transgenic mice demonstrate AP-1 (activator protein-1) transactivation is required for tumor promotion. *Proc Natl Acad Sci U S A.* 1999;96(17):9827-9832.
15. Eferl R, Wagner EF. AP-1: a double-edged sword in tumorigenesis. *Nat Rev Cancer.* 2003;3(11):859-868.
16. Bakiri L, Lallemand D, Bossy-Wetzel E, Yaniv M. Cell cycle-dependent variations in c-Jun and JunB phosphorylation: a role in the control of cyclin D1 expression. *EMBO J.* 2000;19(9):2056-2068.
17. Eferl R, Ricci R, Kenner L, et al. Liver tumor development. c-Jun antagonizes the proapoptotic activity of p53. *Cell.* 2003;112(2):181-192.
18. Kasibhatla S, Brunner T, Genestier L, Echeverri F, Mahboubi A, Green DR. DNA damaging agents induce expression of Fas ligand and subsequent apoptosis in T lymphocytes via the activation of NF-kappa B and AP-1. *Mol Cell.* 1998;1(4):543-551.
19. Raitano AB, Halpern JR, Hambuch TM, Sawyers CL. The Bcr-Abl leukemia oncogene activates Jun kinase and requires Jun for transformation. *Proc Natl Acad Sci U S A.* 1995;92(25):11746-11750.
20. Burgess GS, Williamson EA, Cripe LD, et al. Regulation of the c-jun gene in p210 BCR-ABL–transformed cells corresponds with activity of JNK, the c-jun N-terminal kinase. *Blood.* 1998;92(7):2450-2460.
21. Hess P, Pihan G, Sawyers CL, Flavell RA, Davis RJ. Survival signaling mediated by c-Jun NH(2)-terminal kinase in transformed B lymphoblasts. *Nat Genet.* 2002;32(1):201-205.
22. Gururajan M, Chui R, Karuppannan AK, Ke J, Jennings CD, Bondada S. c-Jun N-terminal kinase (JNK) is required for survival and proliferation of B-lymphoma cells. *Blood.* 2005;106(4):1382-1391.
23. Knoepfler PS, Zhang XY, Cheng PF, Gafken PR, McMahon SB, Eisenman RN. Myc influences global chromatin structure. *EMBO J.* 2006;25(12):2723-2734.
24. Esteller M. Cancer epigenomics: DNA methylomes and histone-modification maps. *Nat Rev Genet.* 2007;8(4):286-298.
25. Jones PA, Baylin SB. The epigenomics of cancer. *Cell.* 2007;128(4):683-692.
26. Suzuki MM, Bird A. DNA methylation landscapes: provocative insights from epigenomics. *Nat Rev Genet.* 2008;9(6):465-476.
27. Behrens A, Sibilia M, David JP, et al. Impaired postnatal hepatocyte proliferation and liver regeneration in mice lacking c-jun in the liver. *EMBO J.* 2002;21(7):1782-1790.
28. Rickert RC, Roes J, Rajewsky K. B lymphocyte-specific, Cre-mediated mutagenesis in mice. *Nucleic Acids Res.* 1997;25(6):1317-1318.
29. Sabapathy K, Kallunki T, David JP, Graef I, Karin M, Wagner EF. c-Jun NH2-terminal kinase (JNK)1 and JNK2 have similar and stage-dependent roles in regulating T cell apoptosis and proliferation. *J Exp Med.* 2001;193(3):317-328.
30. Behrens A, Sibilia M, Wagner EF. Amino-terminal phosphorylation of c-Jun regulates stress-induced apoptosis and cellular proliferation. *Nat Genet.* 1999;21(3):326-329.
31. Donehower LA, Harvey M, Slagle BL, et al. Mice deficient for p53 are developmentally normal but susceptible to spontaneous tumours. *Nature.* 1992;356(6366):215-221.
32. Malumbres M, Sotillo R, Santamaria D, et al. Mammalian cells cycle without the D-type cyclin-dependent kinases Cdk4 and Cdk6. *Cell.* 2004;118(4):493-504.
33. Shinkai Y, Rathbun G, Lam KP, et al. RAG-2-deficient mice lack mature lymphocytes owing to inability to initiate V(D)J rearrangement. *Cell.* 1992;68(5):855-867.
34. Sexl V, Piekorz R, Moriggl R, et al. Stat5a/b contribute to interleukin 7-induced B-cell precursor expansion, but abl- and bcr/abl-induced transformation are independent of stat5. *Blood.* 2000;96(6):2277-2283.
35. Ott RG, Simma O, Kollmann K, et al. JunB is a gatekeeper for B-lymphoid leukemia. *Oncogene.* 2007;26(33):4863-4871.
36. Kerenyi MA, Grebien F, Gehart H, et al. Stat5 regulates cellular iron uptake of erythroid cells via IRP-2 and TfR-1. *Blood.* 2008;112(9):3878-3888.
37. Li LC, Dahiya R. MethPrimer: designing primers for methylation PCRs. *Bioinformatics.* 2002;18(11):1427-1431.
38. Unnikrishnan I, Radfar A, Jenab-Wolcott J, Rosenberg N. p53 mediates apoptotic crisis in primary Abelson virus-transformed pre-B cells. *Mol Cell Biol.* 1999;19(7):4825-4831.
39. Hoelbl A, Schuster C, Kovacic B, et al. Stat5 is indispensable for the maintenance of bcr/abl-positive leukaemia. *EMBO Mol Med.* 2010;2(3):98-110.
40. Okano M, Xie S, Li E. Cloning and characterization of a family of novel mammalian DNA (cytosine-5) methyltransferases. *Nat Genet.* 1998;19(3):219-220.
41. Okano M, Bell DW, Haber DA, Li E. DNA methyltransferases Dnmt3a and Dnmt3b are essential for de novo methylation and mammalian development. *Cell.* 1999;99(3):247-257.
42. Robertson KD, Uzvolgyi E, Liang G, et al. The human DNA methyltransferases (DNMTs) 1, 3a and 3b: coordinate mRNA expression in normal tissues and overexpression in tumors. *Nucleic Acids Res.* 1999;27(11):2291-2298.
43. Chilosi M, Doglioni C, Yan Z, et al. Differential expression of cyclin-dependent kinase 6 in cortical thymocytes and T-cell lymphoblastic lymphoma/leukemia. *Am J Pathol.* 1998;152(1):209-217.
44. Lien HC, Lin CW, Huang PH, Chang ML, Hsu SM. Expression of cyclin-dependent kinase 6 (cdk6) and frequent loss of CD44 in nasal-

nasopharyngeal NK/T-cell lymphomas: comparison with CD56-negative peripheral T-cell lymphomas. *Lab Invest.* 2000;80(6):893-900.

45. Schwartz R, Engel I, Fallahi-Sichani M, Petrie HT, Murre C. Gene expression patterns define novel roles for E47 in cell cycle progression, cytokine-mediated signaling, and T lineage development. *Proc Natl Acad Sci U S A.* 2006;103(26):9976-9981.
46. Nagel S, Leich E, Quentmeier H, et al. Amplification at 7q22 targets cyclin-dependent kinase 6 in T-cell lymphoma. *Leukemia.* 2008;22(2):387-392.
47. Brito-Babapulle V, Gruszka-Westwood AM, Platt G, et al. Translocation t(2;7)(p12;q21-22) with dysregulation of the CDK6 gene mapping to 7q21-22 in a non-Hodgkin's lymphoma with leukemia. *Haematologica.* 2002;87(4):357-362.
48. Hayette S, Tigaud I, Callet-Bauchu E, et al. In B-cell chronic lymphocytic leukemias, 7q21 translocations lead to overexpression of the CDK6 gene. *Blood.* 2003;102(4):1549-1550.
49. Chen D, Law ME, Theis JD, et al. Clinicopathologic features of CDK6 translocation-associated B-cell lymphoproliferative disorders. *Am J Surg Pathol.* 2009;33(5):720-729.
50. Agirre X, Vilas-Zornoza A, Jimenez-Velasco A, et al. Epigenetic silencing of the tumor suppressor microRNA Hsa-miR-124a regulates CDK6 expression and confers a poor prognosis in acute lymphoblastic leukemia. *Cancer Res.* 2009;69(10):4443-4453.